Stopping power in the independent-particle model: Harmonic oscillator results

R. Cabrera-Trujillo*
Departamento de Física, Universidad Autónoma Metropolitana-Iztapalapa, Apartado Postal 55-534, 09340 México Distrito Federal, México

(Received 23 October 1998; revised manuscript received 5 April 1999)

Electronic stopping cross sections for atoms and molecules in the gas phase have been evaluated within the independent-particle model for the range of velocities where the first Born approximation is valid for targets with $Z_2 \leqslant 18$. It is shown that in this approximation, the electronic stopping power is expressed as a Bragg sum rule. In the case that the target electron is considered as harmonically bound, the stopping cross section is obtained in an analytical form depending solely on the frequency of the electron. Using the virial theorem, a relation is found between the harmonic oscillator frequency and the electronic properties of the target, such that the stopping power is described in a self-contained way. The results are compared with other theoretical treatments and with available experimental data. For the case of projectiles with structure, I use the results for the effective charge (screening effect) of Cabrera-Trujillo, Cruz, Oddershede, and Sabin [Phys. Rev. A **55**, 2864 (1997)]. From the analytical expression for S_e, one obtains the shell contributions to the electronic stopping cross section, finding that in this model, shell corrections also come from considering the whole set of allowed excitations in the target with a dependence on the orbital mean excitation energy and the projectile mass. [S1050-2947(99)09309-9]

PACS number(s): 34.50.Bw

I. INTRODUCTION

The interaction of swift, massive particles with matter is a field with implications for such diverse studies as astrophysics, nuclear and atomic physics, ion beam implantation of impurities in solids, and radiation therapy, to mention just a few. When a particle makes its way through a substance, its interaction with surrounding atoms and molecules leads to the transfer of part of its energy to the medium.

In 1930 Bethe [1] established the quantum theory for energy loss of a point charge when it penetrates a medium. According to Bethe's theory [1], the electronic stopping cross section (S_e) in the first Born approximation for a swift stripped ion with charge Z_1 colliding with a target with N_2 bound electrons is given by

$$S_e(v) = \frac{4\pi e^4 Z_1^2 N_2}{m_e v^2}\left\{\ln\left(\frac{2m_e v^2}{I_0}\right) - \frac{C(v)}{N_2}\right\}, \qquad (1.1)$$

valid for the case when the velocity of the projectile, v, is higher than the target electron's velocity v_e. Here $C(v)/N_2$ are the so-called shell corrections for the system and I_0 is the mean excitation energy of the target which is defined in terms of the dipole oscillator strength (DOS) f_{nn_0} [2] as

$$N_2 \ln I_0 = \sum_n f_{nn_0} \ln(E_n - E_{n_0}), \qquad (1.2)$$

with E_{n_0} and E_n denoting the energies of the system in the initial and final states, respectively.

In order to evaluate I_0, the complete DOS distribution of the target must be known, so it may be necessary to resort to approximate methods or—most frequently—to obtain I_0 either semiempirically or from fits of theory to experimental data. Theoretically, in the last few years there have been several approaches to the calculation of stopping power, shell corrections, and mean excitation energies by employing, in several different forms, a decomposition into separate orbital contributions.

Pathak [3] decomposed the stopping into contributions from valence electrons, conduction electrons, and inner-core electrons. On the other hand, Tung and Watt [4] obtained contributions to S_e from the inner shell electrons, by using the local plasma approximation (LPA) of Lindhard and Scharff [5], and from valence electrons by using a dielectric response approach. Oddershede and Sabin (OS) [6–9] have treated shell corrections and mean excitation energies by using the kinetic theory (KT) of stopping [10]. OS found that the KT gives good results *provided* it is used on an orbital-by-orbital basis [6]. This condition includes the use of an orbitally decomposed form of the Bethe logarithmic form, hence requiring orbital mean excitation energies. To this end, OS used the orbital mean excitation energies obtained by Dehmer *et al.* [11] and Inokuti *et al.* [12,13] within the independent-electron model from the Hartree-Slater calculation of the DOS.

On the other hand, Meltzer *et al.* [14,15] proposed an orbital density generalization of the LPA to calculate orbital mean excitation energies. Within the kinetic theory, they calculate stopping cross sections, finding that their results do not differ substantially from those of OS although the two methods were different.

Up to now many of the efforts, including those previously cited, have been based on numerical analyses for all the velocities allowed within the first Born approximation. The aim of this work is to lay the foundation of the use of the

*Present address: Quantum Theory Project, Department of Physics, University of Florida, P. O. Box 118435, Gainesville, FL 32611-8435.

independent-particle model in the calculation of electronic stopping power and to obtain an analytical expression for it. In the first place, I show that in this context the stopping power is separated into contributions from the target orbitals as a Bragg-like rule. Also, for high velocities (low momentum transfer) we obtain an orbital decomposition of the mean excitation energy.

Since the original work by Bethe [1], much effort has been made and several methods have been used in calculating analytical and realistic descriptions for the electronic stopping power. One of them has been the quantal harmonic oscillator (HO) model which is widely used in many branches of physics, such as quantum optics, atomic, molecular, and solid state physics, first because all the excitation spectra and solutions are well known, and second, because to first order it represents the potential of a bound electron.

Recent work [16,17] has shown that the electronic stopping cross section can be evaluated in terms of series or integrals on the basis of a quantal harmonic oscillator model for the atom. However, as Sigmund and Haagerup stated [16], ''in the case of a heavy projectile, $M_1 \gg m_e$, one comes closest to an analytical expression.'' It is within this spirit that I will obtain an analytical expression for S_e, and it will be related to a realistic description of the target.

In Sec. II, I start with a summary of the quantum electronic stopping theory in the first Born approximation. Next, I show the implementation of the independent-particle model and obtain a self-contained analytical result for S_e under the HO approach. In Sec. III, I compare the results of this model with experiment and other theories. In order to compare to the experiment, I use the analytical result for the effective charge (screening effect) of Cabrera-Trujillo *et al.* [18] and I compare the results for the electronic stopping cross section with those of OS and the experimental data available for He, Li, C, and Al. Also, I show the results for the shell corrections and compare them with the OS results, finding a good agreement. Finally, in Sec. IV, I provide some discussion and conclusions as well as remarks concerning further work.

II. THEORY

A. Electronic stopping power

Let us consider a process in which a point charge with velocity v, mass M_1, and nuclear charge $Z_1 e$ collides with a stationary gas phase target with mass M_2 and N_2 bound electrons in an initial state denoted by $|m_0\rangle$. The projectile is deflected into the solid angle element $d\Omega$ along a direction with polar angle θ and azimuthal angle φ, measured in the laboratory frame. Suppose the target undergoes a transition to final states $|m\rangle$; then the kinetic energy of the projectile, when electron transfer is not permitted, is thereby reduced by $E_m - E_{m_0}$.

Following Bethe's classic derivation [2,19], the electronic stopping cross section can be written as

$$S_e(v) = \frac{2Z_1^2 e^4}{m_e v^2} \sum_{m>m_0} \int_{q_{min}}^{q_{max}} F_{mm_0}(\mathbf{q}) \frac{d\mathbf{q}}{q^2}, \qquad (2.1)$$

where $\mathbf{q}$ is the momentum transfer, $d\mathbf{q} = q\,dq\,d\varphi$, and F_{mm_0} are the generalized oscillator strengths (GOSs) given by

$$F_{mm_0}(\mathbf{q}) = \frac{2m_e}{\hbar^2 q^2}(E_m - E_{m_0})|M_{mm_0}(\mathbf{q})|^2, \qquad (2.2)$$

with

$$M_{mm_0}(\mathbf{q}) = \langle m_0 | \sum_{i=1}^{N_2} e^{-i\mathbf{q}\cdot\mathbf{r}_i} | m \rangle \qquad (2.3)$$

being the atomic form factor [20] of the target.

Note that Eqs. (2.1) and (2.3) do not include the integration on the azimuthal angle φ due to the contribution coming from the spatial orientation of the target electronic distribution [21]. The limits of the q integration are determined by the kinematics of the collision process and they are given by [22]

$$q_{min}^{max} = \frac{M_1 v}{\hbar}\left[1 \pm \sqrt{1 - \frac{2(E_m - E_{m_0})}{M_1 v^2}}\right]. \qquad (2.4)$$

Equation (2.1) is a first Born approximation to the electronic stopping power of ions incident on an atomic or molecular target. The GOS terms in Eq. (2.1) give the contribution to the stopping cross section from the target transitions; i.e., each GOS term constitutes the probability that the projectile induces a target transition from the initial state $|m_0\rangle$ to the final state $|m\rangle$ with an absorption of energy $E_m - E_{m_0}$.

B. Independent-electron model

The analysis of Eq. (2.1) requires knowledge of the complete spectrum of excitations and the corresponding wave functions. This knowledge implies solutions of the unperturbed Schrödinger equation for the system of N_2 electrons. However, in reality, this calculation is a difficult task, and one has to resort to approximate solutions. It is in this spirit that we will reformulate the previous results within the independent-particle model. In this situation, the system is described by a Hartree-Fock wave function of the form

$$|m\rangle = |m_1, m_2, \ldots, m_{N_2}|, \qquad (2.5)$$

where $|m_i\rangle$ is a one-electron eigenfunction. Therefore, the energy transfer from the ground state $|m_0\rangle$ to the excited state $|m\rangle$ is given by

$$E_m - E_{m_0} = \sum_{i=1}^{N_2} (E_{m_i} - E_{m_{0i}}), \qquad (2.6)$$

where the subindex m_i stands for the ith electron in the excited state m. From this approach, one can see that for a one-electron operator $O = \Sigma_{j=1}^{N_2} O_j$, the only way we can obtain an atomic form factor different from zero is that the wave function for the excited state differs from that of the ground state by one orbital. Supposing then that the excitation occurs for the jth orbital, the atomic form factor (2.3) becomes

$$M_{m_j m_{0j}}^{(j)} = \langle m_j | O_j | m_{0j} \rangle. \qquad (2.7)$$

Therefore, using these two previous results, one finds that for this one-electron operator, the GOS can be rewritten as the contributions of each individual orbital, i.e., as

$$G_{mm_0}=\sum_{j=1}^{N_2} G^{(j)}_{m_j m_{0j}}, \tag{2.8}$$

where

$$G^{(j)}_{m_j m_{0j}}=(E_{m_j}-E_{m_{0j}})|\langle m_{0j}|O_j|m_j\rangle|^2 \tag{2.9}$$

is the orbital contribution in the independent-particle model.

In the particular case in which the one-electron operator is given by the plane wave, $O_j=e^{-i\mathbf{q}\cdot\mathbf{r}_j}$, the orbital GOS becomes

$$F^{(j)}_{m_j m_{0j}}(\mathbf{q})=\frac{2m_e}{\hbar^2 q^2}(E_{m_j}-E_{m_{0j}})|\langle m_{0j}|e^{-i\mathbf{q}\cdot\mathbf{r}_j}|m_j\rangle|^2. \tag{2.10}$$

From this result and Eq. (2.1) we can observe immediately that the stopping cross section is given by

$$S_e(v)=\sum_i S_{e,i}(v), \tag{2.11}$$

where

$$S_{e,i}(v)=\frac{2e^4Z_1^2}{m_e v^2}\sum_{m_i}\int_{q_{min,i}}^{q_{max,i}} F^{(i)}_{m_i m_{0i}}(\mathbf{q})\frac{d\mathbf{q}}{q^2} \tag{2.12}$$

is the contribution of the ith orbital. This result resembles Bragg and Kleeman's rule [23] for the stopping cross section, which states that ''the total stopping cross section is the weighted sum of the atomic stopping cross sections $S_{e,i}$, where the weight factors are the numbers of atoms of type i'' but in this case reformulated orbital by orbital.

Note the limits of integration. From Eq. (2.7) and kinematic considerations, the limits on the transferred momentum take into account only the energy transferred to this orbital, i.e., $E_{m_j}-E_{m_{0j}}$. We will analyze in more detail the importance of this result in Secs. III and IV. For the moment, we will use the Bethe approximation for high velocities.

C. Bethe approximation

Following the classic derivation of the Bethe formula [2], in Eq. (2.12) one uses the fact that for high velocities the limits of the q integration are determined by the kinematics of the binary collision process; therefore for heavy ions [2]

$$q_{max,i}=\frac{2m_e v}{\hbar},\quad q_{min,i}=\frac{E_{m_i}-E_{m_{0i}}}{\hbar v}. \tag{2.13}$$

Following Bethe [2], one exchanges the summation over m_i in Eq. (2.12) with the integration, and since the only term that depends on the excited state is $q_{min,i}$, it is replaced by a suitably averaged value which is independent of the excitation state:

$$q_{min,i_{AV}}=\frac{I_{0i}}{\hbar v}. \tag{2.14}$$

Using this approximation and the Bethe sum rule fulfilled by the GOS [1],

$$\sum_{m_j} F^{(j)}_{m_j m_{0j}}(\mathbf{q})=1, \tag{2.15}$$

we obtain the result that

$$S_{e,i}(v)=\frac{2e^4Z_1^2}{m_e v^2}\int_{q_{min,i_{AV}}}^{q_{max,i}}\frac{d\mathbf{q}}{q^2}=\frac{4\pi e^4Z_1^2}{m_e v^2}\ln\left(\frac{2m_e v^2}{I_{0i}}\right), \tag{2.16}$$

which is the standard Bethe result [see Eq. (1.1)], where I_{0i} is defined through the dipole oscillator strength $f^{(i)}_{m_i m_{0i}}=\lim_{q\to 0}F^{(i)}_{m_i m_{0i}}(\mathbf{q})$ as

$$\ln I_{0i}=\sum_{m_i} f^{(i)}_{m_i m_{0i}}\ln(E_{m_i}-E_{m_{0i}}). \tag{2.17}$$

Therefore, from Eq. (2.11), one sees that in the high-velocity regime

$$N_2\ln I_0=\sum_{i=1} n_i\ln I_{0i}, \tag{2.18}$$

where n_i is the occupation number of the orbital i.

This equation is precisely the Bragg-like rule decomposition for the mean excitation energy of a complex system [24]. Let me note that the meaning of I_0 has sense only in the high-velocity region. In the intermediate- to low-velocity region, the orbital mean excitation energy I_{0i} is the one which will describe more realistically the stopping as has been found previously by OS [6].

D. Harmonic oscillator model implementation

In order to derive an analytical expression for the stopping cross section $S_e(v)$, I will assume that each electron of the target is bound harmonically [25] with its own force constant.

For a spherical three-dimensional harmonic oscillator with a natural frequency ω_{0i}, the wave function is given by

$$\phi_{m_i}=A_{m_i}e^{-\alpha_i^2(x_i^2+y_i^2+z_i^2)/2}\prod_{x=x,y,z}H_{m_{ix}}(\alpha_i x_i), \tag{2.19}$$

where A_{m_i} is the normalization constant for that orbital, the $H_{m_{ix}}$ are the Hermite polynomials, $\alpha_i^2=m_e\omega_{0i}/\hbar$, and the unperturbed orbital energy is given by

$$E_{m_i}=\hbar\omega_{0i}\left(m_{ix}+m_{iy}+m_{iz}+\frac{3}{2}\right).$$

Since the wave function is spherically symmetric, I will suppose that the momentum transfer takes place along the z direction, such that the only contributing state is m_{iz} and the atomic form factor for the jth electron is calculated in a straightforward way from Eq. (2.7), resulting in

$$M^{(j)}_{m_j m_{0j}}(\mathbf{q}) = \frac{2^{m_j/2}}{\sqrt{m_j!}}\left(\frac{iq}{2\alpha_j}\right)^{m_j} e^{-q^2/4\alpha_j^2}, \tag{2.20}$$

where $m_j = m_{jz}$. Here, I have assumed that the ground state is for $m_{0i}=0$. Therefore the GOS for the jth orbital is given by

$$F^{(j)}_{m_j m_{0j}}(\mathbf{q}) = \frac{1}{(m_j-1)!}\left(\frac{q^2}{2\alpha_j^2}\right)^{m_j-1} e^{-q^2/2\alpha_j^2}, \tag{2.21}$$

which by direct calculation is seen to satisfy the Bethe sum rule [Eq. (2.15)]. Inserting Eq. (2.21) into the definition of the orbital electronic stopping cross section [Eq. (2.12)], one obtains

$$S_{e,i}(v) = \frac{4\pi e^4 Z_1^2}{m_e v^2} L_i(v), \tag{2.22}$$

where $L_i(v)$ is called the orbital stopping number, given by

$$L_i(v) = \frac{1}{2}\left\{ \mathrm{Ei}(x)\Big|_{x_{min}(1)}^{x_{max}(1)} - e^{-x}\Big|_{x_{min}(2)}^{x_{max}(2)} - \sum_{\nu=3}^{[E_p/I_{0i}]} e^{-x}\left[\frac{x^{\nu-2}}{(\nu-1)!} + \sum_{k=1}^{\nu-2}\frac{x^{\nu-k-2}}{(\nu-1)(\nu-k-2)!}\right]\Big|_{x_{min}(\nu)}^{x_{max}(\nu)}\right\}, \tag{2.23}$$

where $\mathrm{Ei}(x)$ is the exponential integral function [26], which is defined as

$$\mathrm{Ei}(x) = \gamma + \ln x + \sum_{k=1}^{\infty}\frac{(-1)^k x^k}{k k!}.$$

Here $\gamma = 0.577\,215\,66$, the Euler constant, and

$$x^{max}_{min}(\nu_i) = \frac{M_1^2 v^2}{2m_e\hbar\omega_{0i}}\left(1 \pm \sqrt{1 - \frac{2\hbar\omega_{0i}\nu_i}{M_1 v^2}}\right)^2. \tag{2.24}$$

As one sees, this is an analytical and exact result for the stopping cross section, within the first Born approximation for a quantal harmonic oscillator.

E. High-velocity limit

Let me analyze Eq. (2.22) for the case where the projectile collides with a velocity higher than the electron velocity. In this case, from Eq. (2.24),

$$x_{max}(\nu_i) = \frac{2M_1^2 v^2}{m_e\hbar\omega_{0i}} \gg 1,$$

$$x_{min}(\nu_i) = \frac{\hbar\omega_{0i}\nu_i^2}{2m_e v^2} \ll 1, \tag{2.25}$$

such that one can use the asymptotic formulas for the exponential integral function [26],

$$\mathrm{Ei}(z) \sim \ln z, \quad z \ll 1,$$

$$\mathrm{Ei}(z) \sim \frac{e^{-z}}{z}\left[1 - \frac{1}{z}\right], \quad z \gg 1, \tag{2.26}$$

which when used in Eq. (2.22) gives

$$S_{e,i}(v) = \frac{4\pi e^4 Z_1}{m_e v^2}\left\{\ln\left(\frac{2m_e v^2}{\hbar\omega_{0i}}\right) + \sum_j \frac{\epsilon_j(\hbar\omega_{0i}, M_1)}{(v^2)^j}\right\}. \tag{2.27}$$

Here $\epsilon_j(\hbar\omega_{0i}, M_1)$ is the coefficient for the so-called shell corrections which has been given by Sigmund and Haagerup [16]. From this result, one sees that the Bethe term comes from the contribution of the first excited state ($\nu=1$), and the higher excited states contribute to the so-called *shell corrections*. Also, from Eq. (1.1), one can identify the angular frequency of revolution of the ith electron times $\hbar$ as the mean excitation energy — a result similar to that previously found by Kramers [27] for a free electron gas. This result can be obtained from the definition of the orbital mean excitation energy [Eq. (2.17)], calculating directly the DOS as follows. For the HO model we have

$$f^{(i)}_{m_i m_{0i}} = \delta_{m_i 1}, \tag{2.28}$$

contributing only the first excited state. Therefore $E_{i1} - E_{i0} = \hbar\omega_{0i}$, such that the orbital mean excitation energy is given by

$$I_{0i} = \hbar\omega_{0i}.$$

In the next section I will utilize further the above assumptions in order to find a complete description of the target by means of the harmonic oscillator.

F. Revolution frequency and the mean excitation energy

In order to apply the method proposed in this work and provide a proper discussion of the previous results, it is necessary to obtain a realistic description of the angular frequency ω_{0i} of the target electron and therefore a realistic description of the orbital mean excitation energy I_{0i}.

Since we are representing the behavior of an electron by means of a harmonic oscillator wave function, from Eq. (2.19) we see that all the physical information is contained in the parameter ω_{0i}. The way we will relate this parameter to a realistic situation is through the virial theorem.

For one electron represented by a harmonic oscillator wave function, the potential is given by $V_{HO} = m_e\omega_{0i}^2\langle r_i^2\rangle/2$, where $\langle r_i^2\rangle$ is the expectation value of the mean square position in a given realistic basis set.

The virial theorem for a potential of the form r^n reads as

$$\langle T_i\rangle = \frac{n}{2}\langle V_i\rangle. \tag{2.29}$$

Therefore, for the harmonic oscillator potential, $\langle T_i\rangle_{HO} = \langle V_i\rangle_{HO}$, and therefore, $m_e\omega_{0i}^2\langle r_i^2\rangle/2 = \langle T_i\rangle_{HO}$. But if the electron described by a harmonic oscillator wave function is to have Coulombic information, then the expectation value of its kinetic energy should be the same as the one given by

more realistic description, i.e., $\langle T_i\rangle_{HO}=\langle T_i\rangle$, where $\langle T_i\rangle$ is the expectation value for the electron in a Coulombic potential and described by a realistic basis set. For this Coulombic potential, then, the virial theorem establishes that $\langle T_i\rangle=-\langle V_i\rangle/2=-\epsilon_{0i}$, where ϵ_{0i} is the electronic orbital energy for the ith electron. This last step follows from the use of an independent-oscillator scheme for each atomic level. Then one has

$$\omega_{0i}=\sqrt{-\frac{2\epsilon_{0i}}{m_e\langle r_i^2\rangle}}, \tag{2.30}$$

and therefore, the mean excitation energy for this orbital becomes

$$I_{0i}=\sqrt{-\frac{2\hbar^2\epsilon_{0i}}{m_e\langle r_i^2\rangle}}. \tag{2.31}$$

Knowing the expectation value for $\langle r_i^2\rangle$ and the orbital energy ϵ_{0i}, one can get the mean excitation energy for the ith orbital.

The preceding expression is remarkably simple. It reduces to the classical result since for the Coulombic case $\epsilon_{0i}=-m_e\langle v_e^2\rangle/2$ such that $\omega_{0i}=\langle v_e^2\rangle^{1/2}/\langle r_i^2\rangle^{1/2}$. Also, it indicates that the more compact the orbital, the higher will be the mean excitation energy, a result previously found for a Gaussian wave function within the orbital local plasma approximation (OLPA) model [28].

III. ANALYSIS AND DISCUSSION

A. Mean excitation energy

Let me analyze briefly the predictions of the orbital mean excitation energy calculated in this work for some atomic cases and compare with other theoretical calculations. In Table I, I display the orbital values for I_{0i} obtained from Eq. (2.31) for various atomic systems. The expectation values of $\langle r_i^2\rangle$ were obtained by using accurate Hartree-Fock Slater (HFS) atomic wave functions for neutral atoms in the ground state (extended basis set) by Clementi and Roetti [29]. The orbital energies required by Eq. (2.31) have been taken from the latter reference. In the same table are shown the values of Meltzer, Sabin, and Trickey [14] (MST) obtained by means of the OLPA and local-spin-density approximation densities, and the corresponding values for the mean excitation energy from the calculation of OS [9]. It is interesting to note the fair agreement among the three approaches (although the three methods are different) which reveal some systematic features. For $Z_2=2,\ldots,5$ one sees that the HO results are intermediate between the MST and OS models. For $Z_2>5$, one observes that the K-shell values are higher than those of MST. But as has been pointed out by OS, the valence electrons are the ones that make the higher contribution to S_e. Furthermore, one can observe differences in the valence results, but those are smaller than the core results. On the other hand, we observe that all the herein calculated orbital mean excitation energies show a monotonically decreasing trend within the same target in contrast with the corresponding values of MST and OS. This result means that the natural revolution frequency decreases monotonically for the outer orbitals, making the valence electrons those which will produce the higher contributions to S_e.

B. Stopping cross section

Using the quantities given in Table I as input into Eqs. (2.11) and (2.22), one obtains the contribution to S_e as a function of the energy for projectiles incident on selected gaseous atomic targets.

From Eq. (2.24), we see that the velocity of the projectile determines the number of states which will contribute to S_e; i.e., the maximum number of excitations produced by the projectile will be given by

$$\nu=\frac{M_1v^2}{2I_k}=\frac{E_p}{I_k}, \tag{3.1}$$

such that for the same velocity of the projectile, orbitals with larger orbital mean excitation energy (core orbitals) will contribute less.

As examples, I calculate the electronic stopping cross section for proton projectiles incident on He, Li, C, Al, and Ar gaseous targets and compare with the results of Oddershede and Sabin [9] which are based on an orbital decomposition description of the stopping power. Also, for completeness, I include available experimental data for comparison [30–42]. In order to compare with the available experimental data, it is necessary to consider the effect of the projectile charge. To this end, one resorts to the use of the *effective charge* description for the projectile:

$$S_{e,i}(Z_1,v)=[Z_1^*(v)]^2S_{e,i}(Z_1=1,v). \tag{3.2}$$

In doing so it is necessary to take into account a few points which relate specifically to protons. Effective charge is interpreted as a steady-state average over a large number of discrete capture-loss processes [43]. Assuming this, Yarlagadda *et al.* [44] state that ''statistical models are well justified even for the screening of protons ... The screening of a static proton ... has been studies in quantitative detail ... and these studies fully justify use here of a local-density approximation and a statistical model.'' Based on this result, I use the analytical result of Cabrera-Trujillo *et al.* [18] for the effective charge, which is based on the Thomas-Fermi description of the atom with the analytical solution of Tietz [45] and the adiabatic criterion due to Bohr [46,47]. In Fig. 1, I show the effective charge for protons as a function of the proton velocity v/v_0, where v_0 is the Bohr velocity, and compare with the results of Yarlagadda *et al.* [44].

In Figs. 2–6, I show the electronic stopping cross section for protons under three different approaches. I show the results obtained using the assumption that the proton charge is unity through all the velocities where this model is valid (solid line), Eq. (2.22). In addition, I show the results obtained using the criterion of effective charge [18] for the stopping cross section (dashed line) calculated by means of Eqs. (2.22), (3.2), and Eq. (2.23) of Ref. [18]. Also, I show the stopping cross section obtained using the OS values for the orbital mean excitation energies in Eq. (2.22) (dotted line) for comparison with the direct calculation of OS (+) [9].

From these figures one observes several characteristics in the behavior of the electronic stopping cross section when compared to other models and to the experiment. Despite the

TABLE I. Orbital mean excitation energy and electronic ground-state parameters, as required by Eq. (2.31). The orbital mean excitation energies are given in eV.

Atom	Orb.	$\langle r_k^2 \rangle$ (a.u.)	ϵ_k (hartrees)	I_k	I_k^{MST} [a]	I_k^{OS} [b]	Atom	Orb.	$\langle r_k^2 \rangle$ (a.u.)	ϵ_k (hartrees)	I_k	I_k^{MST} [a]	I_k^{OS} [b]
H	1*s*	3.0000	−0.5000	15.70	11.25	14.99		2*s*	0.5711	−3.7676	98.80	56.77	151.05
He	1*s*	1.1847	−0.9179	33.86	33.66	38.83		2*p*	0.5977	−2.2821	75.17	118.75	169.86
Li	1*s*	0.4468	−2.4777	90.58	69.73	109.32		3*s*	12.3976	−0.2530	5.50	6.08	4.45
	2*s*	17.7377	−0.1963	4.05	3.17	3.29	Al	1*s*	0.0195	−58.5010	2109.15	749.74	1373.04
Be	1*s*	0.2330	−4.7327	173.38	113.91	203.78		2*s*	0.4589	−4.9107	125.83	66.87	187.14
	2*s*	8.4264	−0.3093	7.37	7.81	7.32		2*p*	0.4553	−3.2183	102.26	145.18	221.15
B	1*s*	0.1434	−7.6953	281.83	164.39	320.21		3*s*	7.8989	−0.3934	8.58	8.40	9.01
	2*s*	4.7092	−0.4947	12.47	12.14	16.33		3*p*	13.9853	−0.2100	4.72	4.48	4.85
	2*p*	6.1445	−0.3099	8.64	8.07	11.55	Si	1*s*	0.0167	−68.8124	2469.16	841.22	1497.54
C	1*s*	0.0972	−11.3255	415.22	220.78	451.34		2*s*	0.3773	−6.1565	155.39	77.39	226.08
	2*s*	3.0517	−0.7056	18.50	16.93	27.57		2*p*	0.3597	−4.2560	132.32	172.81	278.63
	2*p*	3.7617	−0.4333	13.08	17.19	20.97		3*s*	5.6692	−0.5398	11.87	10.75	14.56
N	1*s*	0.0703	−15.6291	573.70	283.07	590.00		3*p*	8.9838	−0.2970	6.99	9.06	8.87
	2*s*	2.1495	−0.9453	25.51	21.82	41.24	S	1*s*	0.0127	−92.0170	3275.99	1034.70	1733.73
	2*p*	2.5471	−0.5676	18.16	27.59	32.68		2*s*	0.2685	−9.0156	222.90	100.29	308.23
O	1*s*	0.0531	−20.6687	758.58	349.72	729.41		2*p*	0.2423	−6.6937	202.16	231.89	412.71
	2*s*	1.5816	−1.2443	34.12	27.33	56.86		3*s*	3.4288	−0.8859	19.55	15.57	29.40
	2*p*	1.9758	−0.6319	21.75	40.82	46.64		3*p*	5.1690	−0.4153	10.90	20.06	19.37
F	1*s*	0.0416	−26.3827	968.59	421.58	861.33	Cl	1*s*	0.0112	−104.8847	3722.46	1136.50	1844.43
	2*s*	1.2162	−1.5725	43.74	32.80	74.04		2*s*	0.2312	−10.6078	260.56	112.49	349.09
	2*p*	1.5443	−0.7300	26.45	54.78	62.86		2*p*	0.2043	−8.0725	241.79	263.31	489.36
Ne	1*s*	0.0335	−32.7725	1203.68	497.75	982.68		3*s*	2.8123	−1.0731	23.76	17.99	38.91
	2*s*	0.9672	−1.9304	54.35	38.35	92.22		3*p*	4.0601	−0.5065	13.59	26.46	25.76
	2*p*	1.2291	−0.8504	32.00	70.81	81.37	Ar	1*s*	0.0100	−118.6104	4197.87	1241.21	1948.72
Na	1*s*	0.0275	−40.4785	1476.32	577.82	1110.36		2*s*	0.2012	−12.3222	301.02	125.13	388.29
	2*s*	0.7315	−2.7970	75.22	47.12	119.24		2*p*	0.1743	−9.5715	285.01	295.87	572.56
	2*p*	0.8221	−1.5181	52.27	93.51	124.41		3*s*	2.3505	−1.2773	28.36	20.53	49.93
	3*s*	20.6995	−0.1821	3.61	2.98	2.46		3*p*	3.3110	−0.5910	16.25	33.17	32.95
Mg	1*s*	0.0230	−49.0316	1777.74	661.87	1243.15							

[a]Reference [14].
[b]Reference [9].

fact that the approaches followed by OS and the HO model are different, we note a close agreement between the results obtained for S_e. This outcome is even more remarkable when one uses the orbital mean excitation energies I_{0i} reported by OS [9] in Eq. (2.22) and compare with their results. From this result one can argue that the kinetic theory, with a resulting Bethe logarithmic form for S_e treating scatterers at rest, takes into account, in part, the excited states with the entire transfer momentum, as done by the whole solution of the harmonic oscillator.

On the other hand, we note a small difference in S_e, principally in the region around the maximum of the stopping curve for the case of the bare proton, for the HO results when compared with the OS results. This difference is due to the approach used in calculating I_{0i}, since in this case, one obtains I_{0i} through the virial theorem for a HO wave function, whereas OS use a procedure based on the numerical Hartree-Slater calculation for the orbital oscillator strength by Dehmer and co-workers [11–13].

Also, when one considers the effective charge of the proton, one sees the fair agreement between this approach and the experimental data, principally in the region around the maximum of S_e and higher energies. This feature can be observed for all the cases shown, except helium. A possible explanation is due to the high ionization potential for the helium electrons, since it is more difficult to take out electrons from helium which would screen the proton charge. With this approach, one should take into account the effective charge in a more realistic way; i.e., one must consider the effect of excitations on the projectile and target [18] and charge exchange since it depends on both target and projectile [48], as well as the Barkas and Bloch corrections and higher orders in the Born approximation, which are important for the low-energy region.

C. Shell corrections

Another effect that can be analyzed from this model is the so-called shell corrections. From Eq. (1.1) we see that the shell corrections can be calculated as

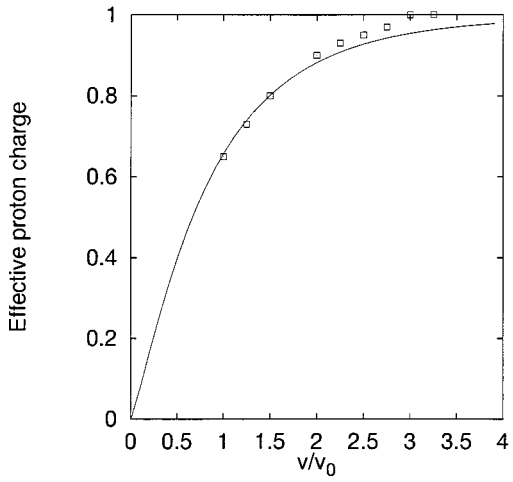

FIG. 1. Effective proton charge. Solid line: results obtained using the model of Cabrera-Trujillo *et al.* [18] and compared with the data taken from Yarlagadda *et al.* [44] (□).

$$\frac{C(v)}{N_2}=\ln\left(\frac{2m_e v^2}{I_0}\right)-\frac{m_e v^2}{4\pi e^4 Z_1^2 N_2}S_e(v) \tag{3.3}$$

for the total contribution of S_e or in a similar way for each orbital contribution $S_{e,i}$, by means of Eq. (2.22). In Fig. 7, I show the shell corrections using Eqs. (2.11) and (2.22) and compare them with the results from OS obtained through the kinetic theory implementation of the electronic stopping cross section [9].

As one can see, the results are in reasonable agreement when compared with the results of the OS model. From this figure, one observes the effect of the orbital decomposition for the stopping cross section, since for the case of C one notes the shell contribution on S_e.

Analyzing Eq. (2.22), one observes two important facts. First, the shell corrections are due not only to the fact that the projectile moves with a velocity comparable to the electron velocity, since this information is included, in part, in the wave function, but also to the fact of considering the whole set of excitations as can be seen from the contribution of Eq. (2.22) for the excited states $\nu \geqslant 3$; i.e., shell corrections are due also to the contribution of the excited states. Second, the effect of considering the whole momentum transfer for low velocities is important, since its contribution to the shell corrections would be higher for lower velocities [see Eq. (2.24)]. Also, since the shell corrections come from the contribution of the excited states evaluated with Eq. (2.24), they will depend on the orbital mean excitation energy I_{0i} and on

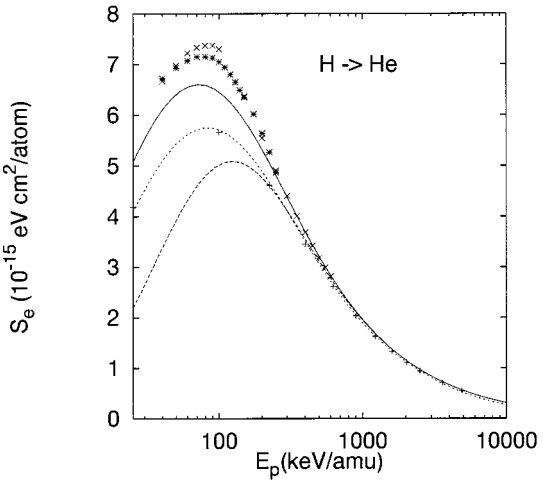

FIG. 2. Comparison of the electronic stopping cross section S_e for protons on atomic helium. Solid line: harmonic oscillator model, Eq. (2.22) and Eq. (2.31). Dashed line: S_e with effective charge, Eq. (3.2). Dotted line: HO result using the OS value of Ref. [9]. (+) Kinetic theory results of OS [9]. Experimental data of Reynolds *et al.* (×) [30] and Park and Zimmerman (∗) [31].

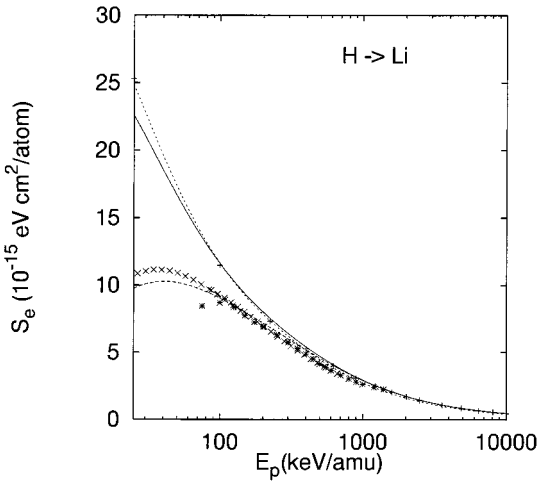

FIG. 3. As in Fig. 2, for Li. Experimental results from Eppacher *et al.* (×) [34] and Bader *et al.* (*) [35].

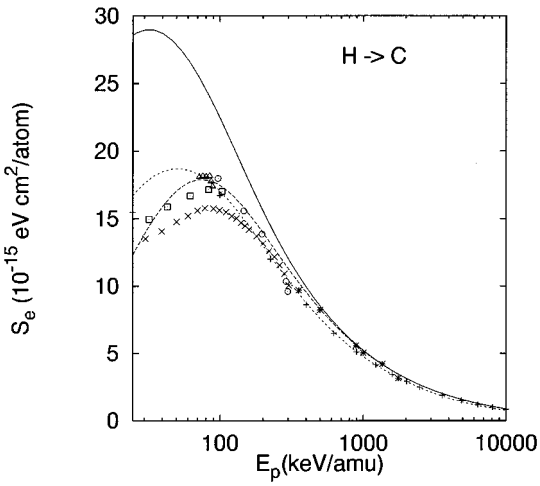

FIG. 4. As in Fig. 2, for C. Experimental results from Mertens and Krist (× and □) [36,37], Ophel and Kerr (∗) [51], Johansen *et al.* (△) [38], and Nyaiesh *et al.* (○) [39].

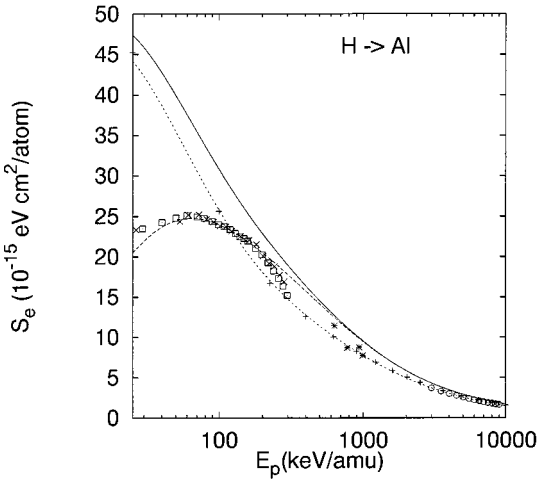

FIG. 5. As in Fig. 2, for Al. Experimental results from Ishiwari *et al.* (×) [40], Kido and Hioki (*) [41], Krist and Mertens (□) [42], and Mertens and Krist (○) [36].

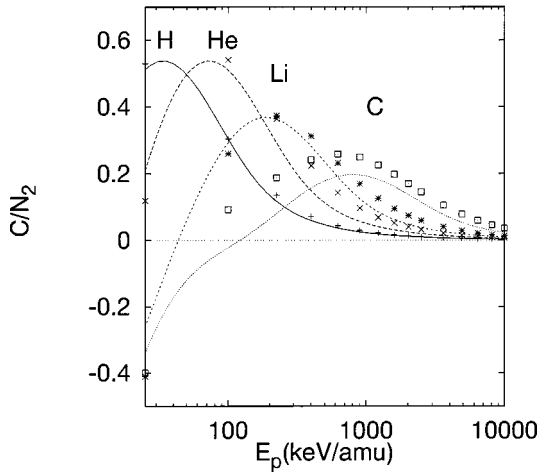

FIG. 7. Comparison of shell correction C/N_2 in the electronic stopping cross section S_e for several atomic targets in this model with the kinetic theory results from OS [9] (+ H, × He, * Li, and □ C).

the projectile mass. This projectile mass feature is discussed in more detail in Ref. [49].

IV. CONCLUSIONS

In the last few years, several efforts have been done to calculate stopping cross sections by employing a decomposition into the separate orbital contributions. Some of these efforts have been discussed in Sec. I.

In this work, I have shown that the electronic stopping cross section is decomposed into a Bragg-like sum under the assumption of describing the target (in the gas phase) as a collection of independent particles. As a consequence of this method, for high projectile energies the Bethe approximation leads to a Bragg-like decomposition for the mean excitation energy I_0.

Using a harmonic oscillator approach for the bound electrons of the target, an analytical expression for the electronic stopping cross section in the first Born approximation is found when use is made of the results for the electronic stopping cross section in the independent-particle model.

Under this assumption, the electronic stopping cross section is realistic, providing a good description of the natural revolution frequency ω_{0i} of the harmonic oscillator by means of realistic wave functions through the virial theorem. Within this approach, I compare with the theoretical result of OS and MST for the orbital mean excitation energy. This approach allows one to calculate the electronic stopping cross section in a self-contained way. When comparing to other theoretical models, one finds a good description of the energy loss, principally for the intermediate- and high-energy regions of the stopping curve. As a consequence of the charge effect in the intermediate- to low-energy region, it is necessary to resort to the inclusion of effective charge. This step allows one to compare S_e with some experimental data, finding a fair agreement.

Also, shell corrections are well described in this approach. One finds that—in contrast to other approaches (see, for example, Ref. [50])—the shell corrections also arise as a consequence of taking into account all the allowed excitations in the target and considering the complete transferred momentum for the collision. This feature is dependent on the mean excitation energy for the orbital and the projectile mass.

Let me note some important considerations in this work. The results shown in this work are based on the first Born approximation, without considering Barkas or Bloch corrections (second Born approximation) in the low-energy region. Also, the method of formulating the charge state of the projectile is still inadequate, since it is necessary to consider excitations and charge exchange in the system of projectile and target. All of this additional work is in progress.

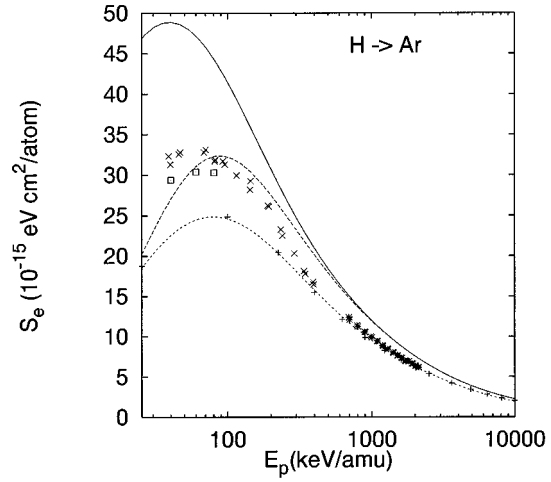

FIG. 6. As in Fig. 2, for Ar. Experimental data of Weyl [52] (×), Reiter *et al.* [53] (*), and Ormrod [54] (□).

ACKNOWLEDGMENTS

The author would like to acknowledge S. A. Cruz, L. E. Porter, J. R. Sabin, and S. B. Trickey for their constructive comments on the manuscript. The work was supported by CONACyT.

[1] H. A. Bethe, Ann. Phys. (Leipzig) **5**, 325 (1930).
[2] H. A. Bethe and R. Jackiw, *Intermediate Quantum Mechanics* (Benjamin/Cummings, New York, 1986).
[3] A. P. Pathak, Phys. Status Solidi B **71**, 35 (1975).
[4] C. J. Tung and D. E. Watt, Radiat. Eff. **90**, 177 (1985).
[5] J. Lindhard and M. Scharff, K. Dan. Vidensk. Selsk. Mat. Fys. Medd. **27**, No. 15, 1 (1953).
[6] J. R. Sabin and J. Oddershede, Phys. Rev. A **26**, 3209 (1982).
[7] J. Oddershede, J. R. Sabin, and P. Sigmund, Phys. Rev. Lett. **51**, 1332 (1983).
[8] J. R. Sabin and J. Oddershede, Phys. Rev. A **29**, 1757 (1984).
[9] J. Oddershede and J. R. Sabin, At. Data Nucl. Data Tables **31**, 275 (1984).
[10] P. Sigmund, Phys. Rev. A **26**, 2497 (1982).
[11] J. L. Dehmer, M. Inokuti, and R. P. Saxon, Phys. Rev. A **12**, 102 (1975).
[12] M. Inokuti, T. Baer, and J. L. Dehmer, Phys. Rev. A **17**, 1229 (1978).
[13] M. Inokuti, J. Dehmer, T. Baer, and J. D. Hanson, Phys. Rev. A **23**, 95 (1981).
[14] D. E. Meltzer, J. R. Sabin, and S. B. Trickey, Phys. Rev. A **41**, 220 (1990).
[15] D. E. Meltzer, J. R. Sabin, S. B. Trickey, and J. Z. Wu, Nucl. Instrum. Methods Phys. Res. B **82**, 493 (1993).
[16] P. Sigmund and U. Haagerup, Phys. Rev. A **34**, 892 (1986).
[17] H. H. Mikkelsen and H. Flyvbjerg, Phys. Rev. A **45**, 3025 (1992).
[18] R. Cabrera-Trujillo, S. A. Cruz, J. Oddershede, and J. R. Sabin, Phys. Rev. A **55**, 2864 (1997).
[19] D. R. Bates, *Atomic and Molecular Processes* (Academic, New York, 1962).
[20] R. W. James, in *The Optical Principles of the Diffraction of X-rays*, edited by L. Bragg (G. Bell and Sons Ltd., London, 1967), p. 109.
[21] H. H. Mikkelsen, J. Oddershede, J. R. Sabin, and E. Bonderup, Nucl. Instrum. Methods Phys. Res. B **100**, 451 (1995).
[22] M. Inokuti, Rev. Mod. Phys. **43**, 297 (1971).
[23] W. H. Bragg and R. Kleeman, Philos. Mag. **10**, 318 (1905).
[24] J. Oddershede and J. Sabin, Int. J. Quantum Chem., Quantum Chem. Symp. **23**, 557 (1989).
[25] N. Bohr, Philos. Mag. **25**, 10 (1913).
[26] *Handbook of Mathematical Functions*, edited by M. Abramowitz and I. A. Stegun (Dover, New York, 1972).
[27] H. A. Kramers, Physica (Amsterdam) **13**, 401 (1947).
[28] R. Cabrera-Trujillo, S. Cruz, and J. Soullard, Nucl. Instrum. Methods Phys. Res. B **94**, 166 (1994).
[29] E. Clementi and C. Roetti, At. Data Nucl. Data Tables **14**, 177 (1974).
[30] H. K. Reynolds, D. N. Dunbar, W. A. Wenzel, and W. Whaling, Phys. Rev. **92**, 742 (1953).
[31] J. T. Park and E. J. Zimmerman, Phys. Rev. **131**, 1611 (1963).
[32] R. Golser and D. Semrad, Phys. Rev. Lett. **66**, 1831 (1991).
[33] R. Golser and D. Semrad, Nucl. Instrum. Methods Phys. Res. B **69**, 18 (1992).
[34] C. Eppacher, R. Diez-Muino, D. Semrad, and A. Arnau, Nucl. Instrum. Methods Phys. Res. B **96**, 639 (1995).
[35] M. Bader, R. E. Pixley, F. S. Mozer, and W. Whaling, Phys. Rev. **103**, 32 (1956).
[36] P. Mertens and T. Krist, Nucl. Instrum. Methods Phys. Res. **194**, 57 (1982).
[37] P. Mertens and T. Krist, Nucl. Instrum. Methods **168**, 33 (1980).
[38] A. Johansen, S. Steenstrup, and T. Wohlenberg, Radiat. Eff. **8**, 31 (1971).
[39] A. R. Nyaiesh, W. Steckelmacher, and M. W. Lucas, J. Phys. C **11**, 2917 (1978).
[40] R. Ishiwari, N. Shiomi-Tsuda, and N. Sakamoto, Nucl. Instrum. Methods Phys. Res. B **35**, 118 (1988).
[41] Y. Kido and T. Hioki, Phys. Rev. B **27**, 2667 (1983).
[42] T. Krist and P. Mertens, Nucl. Instrum. Methods Phys. Res. **218**, 821 (1983).
[43] H. Betz, Rev. Mod. Phys. **44**, 465 (1972).
[44] Y. S. Yarlagadda, J. E. Robinson, and W. Brandt, Phys. Rev. B **17**, 3473 (1978).
[45] T. Tietz, J. Chem. Phys. **25**, 789 (1956).
[46] N. Bohr, Phys. Rev. **58**, 654 (1940).
[47] N. Bohr, Phys. Rev. **59**, 270 (1941).
[48] J. M. Anthony and W. A. Lanford, Phys. Rev. A **25**, 1868 (1982).
[49] R. Cabrera-Trujillo, Nucl. Instrum. Methods Phys. Res. B **149**, 228 (1999).
[50] S. P. Ahlen, Rev. Mod. Phys. **52**, 121 (1980).
[51] T. R. Ophel and G. W. Kerr, Nucl. Instrum. Methods **128**, 149 (1975).
[52] P. K. Weyl, Phys. Rev. **91**, 289 (1953).
[53] G. Reiter, N. Kniest, E. Pfaff, and G. Clausnitzer, Nucl. Instrum. Methods Phys. Res. B **44**, 399 (1990).
[54] J. H. Ormrod, Can. J. Phys. **46**, 497 (1968).